Available online at www.sciencedirect.com

ScienceDirect

Procedia CIRP 10 (2013) 203 – 210

www.elsevier.com/locate/procedia

12th CIRP Conference on Computer Aided Tolerancing

Least-squares fit of measured points for square line-profiles

J. Davidson*, S. Savaliya, and Jami J. Shah

Design Automation Laboratory, Department of Mechanical and Aerospace Engineering
Arizona State University, Tempe, Arizona 85282-6106, USA

Abstract

The pseudoinverse of a rectangular matrix is used to compute the least-squares fit of a set of points that have been measured along a line-profile. Tolerances on line profiles are used to control cross-sectional shapes of parts, such as turbine blades. The specified profile is treated as a moving platform of a hypothetical, redundant, and planar in-parallel-actuated robot, and all the measured points are presumed to be fixed in it. The locations of the linear actuators are represented with screw (torsor) coordinates, and these are arranged in a matrix equation that relates the three small displacements of the platform to the corresponding deviations (treated as small displacements) of the measured points. The Moore-Penrose (pseudoinverse) solution uniquely produces displacements of the platform which correspond to the least-squares minimum for the deviations at all of the measured points.

Keywords: Least-squares; regression; pseudoinverse; fit; profile; point-cloud; CMM data reduction

1. Introduction

The objective of dimensional metrology is to check manufactured parts for conformance to tolerance specifications on drawings. The drawings define features, such as planes, cylinders, and profiles, and the associated tolerance specifications define tolerance-zones for each feature [1]. A tolerance-zone sets the limits for manufacturing variations that are permissible for a feature. Modern coordinate measurement machines (CMMs) provide an automated process of inspection that is replacing many traditional manual methods. The CMM measurements made on a part are represented as the coordinates for a large number of points in a 'cloud'. Although direct comparison of the coordinates for a set of points can determine whether or not all fit within a tolerance-zone, a feature representation is more meaningful when monitoring a manufacturing process. For instance, the boundaries of a minimum-zone, or a least-squares fit, of points is informative about the location of the feature in the tolerance-zone, and there is potential to use drift of the location as a monitoring tool. Considerable computation, arranged in computer software, is required to convert the points to a feature.

Existing methods for fitting a feature to a set of measured points are: a one-sided fit, a two-sided fit, or minimum-zone fit, and the least-squares fit. A recent article summarizing conversion algorithms in general is [2]; another is [3]. An example is [4,5] where measured points are converted to minimum-zone features for planes, lines, and cylinders. One measure of conformance is evaluating whether or not points lie in a specified tolerance-zone. Choi and Kurfess [3] present an algorithm that determines if a point-set, when displaced *en masse*, can fit into the intended zone, and in [6] extend this to determine minimum zones. Conversion algorithms that apply to profiles, including surface-profiles, are described in [3] and [7], although all examples presented are for objects having continuous curvature, such as cones, cylinders, and sculptured surfaces.

The focus of this paper is the development of a new computational method for obtaining the least-squares fit

* Corresponding author. Tel.: +001-480-965-3824
. *E-mail address*: j.davidson@asu.edu.

doi:10.1016/j.procir.2013.08.032

of a set of points that have been measured on a square line-profile, one that has both C^1- and C^2-discontinuity. The results will be a transformed location, similar to [6], and size for the line-profile.

The specifications for a raised square profile are shown in Fig. 1. The shape of the square is controlled by the profile tolerance $t = 0.2$ mm relative to the Datums A, B, and C. This specification establishes two boundary squares at each cross-section of the raised profile. One is 0.1 mm larger along every line normal to the surface, and the other is 0.1 mm smaller, according to the Standard [1].

2. Regression line in the plane

To understand better the meaning of the Moore-Penrose inverse, which is used later in the paper, we undertake a straight-line fit of n identified points in a plane. Considering the solution-line to be of the form $y = mx + b$, there are n linear equations that relate the x_i- and y_i-values. From the Gauss-Markov Theorem [8], the least-squares fit is obtained by minimizing the sum

$$\sum\{y_i - (mx_i + b)\}^2 \qquad (1)$$

for $i = 1\ldots n$. As one example, apply simple linear regression to the five points in Table 1 which are symmetrically disposed about the line $y = 1 + x/2$ in the $x_j y_j$-frame in Fig. 2. When standard software (e.g. MAPLE) for linear regression is applied to these five points, the result is $m = 24/53$ and $b = 69/53$. It is shown as the line with long dashes in Fig. 2.

Table 1. Coordinates of points for the example of least-squares fit for a line

Point	1	2	3	4	5
x	3	5	8	8	8
y	3	3	4	5	6

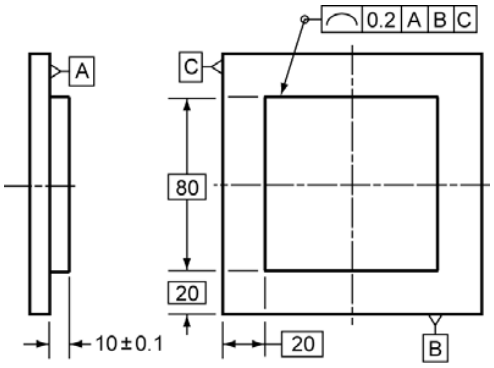

Fig. 1. Specification for a raised profile having sharp corners. Its shape is controlled by the profile tolerance $t = 0.2$ mm relative to Datums A, B, C.

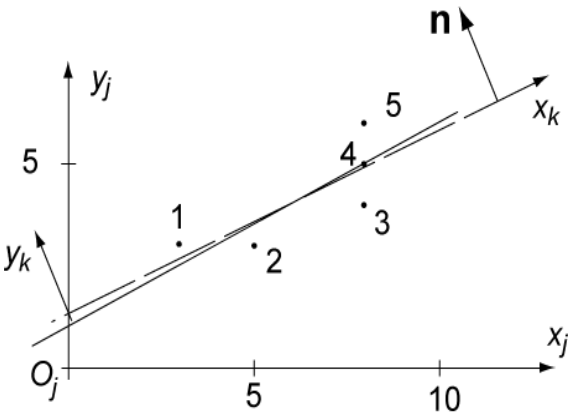

Fig. 2. Five points equally disposed about a line $y = 1 + x/2$ (solid line) in the $x_j y_j$-frame and the standard regression line (dashed line) for them.

The set of n equations, which relate the n points to the linear regression line, may also be written

$$[\mathbf{y}_i] = [\boldsymbol{K}'][\$] = \begin{bmatrix} x_1 & 1 \\ x_2 & 1 \\ \vdots & \vdots \\ x_n & 1 \end{bmatrix} [\$], \qquad (2)$$

where $[\mathbf{y}_i] = [y_1 \ldots y_n]^{\mathsf{T}}$, $[\$] = [m\ b]^{\mathsf{T}}$, and $[\boldsymbol{K}']$ is an $n \times 2$ rectangular coefficient matrix. The n linear equations are, of course, inconsistent. However, they may be solved for the unknowns m and b in [\$] by using one of several *generalized inverses*; these give an *array* of inverse matrices and corresponding solutions for [\$] [9]. Further, a special one of those inverses, the Moore-Penrose inverse $[\boldsymbol{K}']^{\#}$, ensures that the values m and b contained in [\$] correspond to a minimization of the sum of the squares of all the differences $y_i - (mx_i + b)$. The set of y_i-values reside in matrix $[\mathbf{y}_i]$ and the corresponding set of directions for their measurement resides in the rows of $[\boldsymbol{K}']$. For an overconstrained (and inconsistent) set of linear equations, $[\boldsymbol{K}']^{\#}$ is formed [9] as implied in the second of the equations

$$[\$] = [\boldsymbol{K}']^{\#}[\mathbf{y}_i] = \left\{([\boldsymbol{K}']^{\mathsf{T}}[\boldsymbol{K}'])^{-1}[\boldsymbol{K}']^{\mathsf{T}}\right\}[\mathbf{y}_i]. \qquad (3)$$

When coordinates for the five points in the example above are introduced into matrices $[\boldsymbol{K}']$ and $[\mathbf{y}_i]$ of Eq (2), the Moore-Penrose inverse, $[\boldsymbol{K}']^{\#}$, of $[\boldsymbol{K}']$ gives the same values $m = 24/53$ and $b = 69/53$ that arose from the solution using linear regression. For what follows in §5, it is helpful to note here that, when every y_i is increased (or decreased) by the same value ΔS, Eq. (2) produces an

unchanged slope m and a value for b that is increased exactly by ΔS.

Equations (2) and (3) apply to *any* overconstrained set of linear equations and *any* geometric shape. However, to be useful in the setting of manufacturing variations and tolerance-zones, matrix $[\mathbf{y}_i]$ must contain values that are measured with respect to a reference location of the given geometric shape, the rows of matrix $[\boldsymbol{K}']$ must represent the corresponding directions in which the measured y_i-values (deviations) are made, and matrix [$] then contains values that describe the location of the least-squares fit of the geometric shape relative to the same reference location that was used when measuring the deviations y_i. Therefore, in *any* geometric setting for which such equations might arise, Eq (3) relates the deviations of the y_i-values from the least-squares location of the geometric shape. For the special case of linear regression in the plane of Fig. 2, (*i*) the geometric shape is a line, (*ii*) its reference location is the x-axis, (*iii*) its least-squares fit is the regression line, (*iv*) the coordinates m and b in matrix [$] give the relative location of the regression line and the reference line, and (*v*) all the y_i-values are measured at right angles to the (reference) x-axis.

The computed values m = 24/53 and b = 69/53 for the least-squares line in Fig. 2 are not very close to the theoretical values of 1/2 and 1 because the reference direction for error measurement was not made at right angles to the theoretical geometric shape. However, a second iteration may be undertaken from a new reference $x_k y_k$-frame that has its x_k-axis aligned with the first solution (dashed line in Fig. 2). When the matrix $[\mathbf{y}_i]$ in Eqs (2) and (3) is then formed from the y_k-values that are computed from this new reference direction, and when the results are transformed from the $x_k y_k$-frame to the $x_j y_j$-frame, a revised least-squares solution for best-fit of the points emerges: m = 0.496 and b = 1.024. Further, when the reference direction *is* the theoretical line $y = 1 + x/2$ in the $x_j y_j$-frame in Fig. 2, Eq (3) produces values that, when transformed to the $x_j y_j$-frame, are m = 1/2 and b = 1.

3. The Tolerance-map for square line-profiles

The text in this section is a short summary of the developments presented in [10], and Figs. 3(a), 3(b) and 4 are taken from, [10]. A Tolerance-Map (T-Map) is a hypothetical point-space that represents the freedom of a feature in its tolerance-zone. For line-profiles, the manufacturing variations will be represented with the true profile and all allowable profiles parallel to it. Each point in the T-Map corresponds to any one of these parallel profiles or to any one of them that is displaced, yet remains within the tolerance-zone. Four degrees of freedom are required to specify the manufacturing variations of a line-profile, such as any one cross-section of the square boss in Fig. 1. Correspondingly, its T-Map will be four-dimensional (4-D). Therefore, it becomes necessary to choose five of the parallel and/or displaced profiles as basis profiles and to define the T-Map by placing five corresponding basis points $\psi_1 \ldots \psi_5$ to form the vertices of a basis simplex. Five barycentric coordinates $\lambda_1 \ldots \lambda_5$, each one at its basis point ψ_i, then identify any point ψ in the T-Map, and each such point corresponds to one manufacturing variation (one profile) in the tolerance-zone. Since the number of coordinates exceeds the dimension of the space by unity, designers of the space have the freedom to choose one condition among them. Interpretations of the resulting T-Map are simplified when the condition chosen is $\Sigma\lambda_i = 1$ (i = 1…5). The coordinates $\lambda_1 \ldots \lambda_5$ then become the *areal* coordinates of ψ [11].

Of the five basis-profiles required, two will be: ψ_1, the smallest-sized profile, and ψ_2, the largest-sized profile, i.e. the inner and outer boundaries to the tolerance-zone, respectively. These are both locked in place and cannot displace. The remaining basis-profiles are based on displacements of the *middle-sized* square profile, even though the true profile in the design specification may lie at one boundary of the tolerance-zone or be unevenly positioned between both boundaries [1]. Each manufacturing variation for the middle-sized square is represented by its components of eccentricity (translations), e_x and e_y, and its rotational displacement θ. The basis-profiles displaced to the limits $e_x = t/2$ and $e_y = t/2$ in the x- and y-directions are labeled ψ_3 and ψ_4, respectively, and the one rotated counterclockwise the maximum amount $\theta = t/2\,\bar{a}$ is ψ_5 (Fig. 3(a)).

The 3-D T-Map for all the middle-sized square profiles is established with the four basis-points ψ_{12}, ψ_3, ψ_4, and ψ_5 shown in Fig. 3(b). The origin in Fig. 3(b) is labeled ψ_{12} because it represents the undisplaced middle-sized profile (square profile shown with the dashed line in Fig. 3(a)), i.e. the average of the limiting sizes ψ_1 and

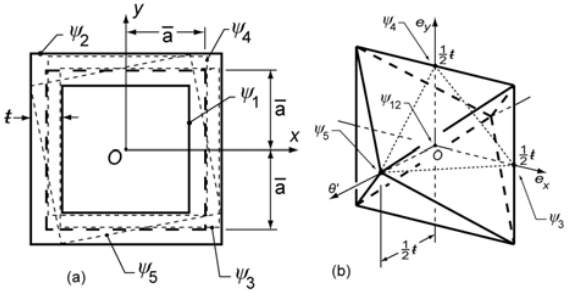

Fig. 3. (a) The middle-sized profile (dashed-lined square) in the (exaggerated) tolerance-zone that is specified with the profile tolerance t; five variational possibilities are labeled, three shown with dotted lines; (b) The T-Map for all the middle-sized squares in the sharp-cornered tolerance-zone of Fig. 3(a). Taken from [10].

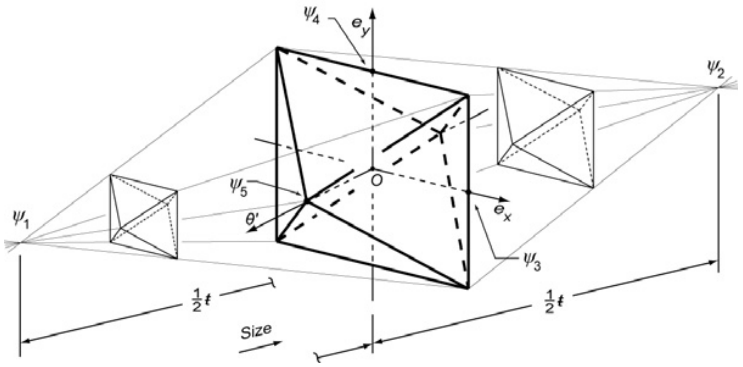

Fig. 4. The 4-D T-Map for the square tolerance-zone in Fig. 3(a) and showing all five basis-points $\psi_1,\ldots,\psi_5$. For clarity of the graphics, the scale in the direction of size ($\psi_1\psi_2$) is exaggerated. Taken from [10] with a minor modification.

ψ_2. Basis-points ψ_3, ψ_4, and ψ_5 are placed at the same distance $t/2$ from the origin along the three axes of a rectangular Cartesian frame of reference with axes e_x, and e_y, and θ'. Note that the angular limit $\theta = t/2\,\overline{a}$ is multiplied by the length $\overline{a}$, i.e. $\theta' = \overline{a}\,\theta$ so that the units along all axes are the same, i.e. a length [L]. Consistent units on all the axes permit the T-Map to be used for metric computations.

It is helpful to view the displacements e_x, and e_y, and θ of the profile to be the same as those of a moveable lamina on which the middle-sized square is etched (dashed line in Fig. 3(a)). For a second location of the lamina, choose one of its fully rotated locations, such as ψ_5 in Fig. 3(a). For these two locations of the lamina, there is a unique point that does not displace. In classic kinematics literature (see e.g. [12]) this point is called the 'pole' of the two locations. For the square profile in Fig. 3(a), the pole is the geometric center (origin O), and it is the point to which the eccentricities e_x and e_y apply in the associated T-Map. Note that the fully rotated profile (and lamina), which is used in defining the pole and its associated origin of the coordinate system Oxy, corresponds to one of the two points in the T-Map where the θ'-axis pierces the boundary (Fig. 3(b)).

Square profiles that are larger or smaller than the middle-sized one are more limited in their allowable displacements e_x, e_y, and θ, and the limits diminish linearly with change in size. Therefore, the full T-Map for the square tolerance-zone in Fig. 3(a) is a double hyperpyramid in 4-D that is depicted in Fig. 4. The base for each single hyperpyramid is the 3-D octahedron from Fig. 3(b), and every other section (two are shown) at right angles to the direction of size is a smaller and geometrically similar octahedron. The combined basis-point ψ_{12}, shown in Fig. 3(b), has been replaced with the individual basis points ψ_1 and ψ_2.

There now is another way to view the objective of this paper: reduce the measured points on one line-profile to a set of small-displacement coordinates that locate a single point within the T-Map of Fig. 4. The result is an *i*-Map, that displays the quality of manufacturing relative to tolerance specifications.

4. Minimum distance between an envelope and a measured point

Every line in the *xy*-plane may be represented with the homogeneous coordinates (*p, q, s*) that may be scaled up or down proportionately without changing the location of the line [see e.g. 13]. Coordinates *p* and *q* are the direction ratios of a normal line that is directed from the origin and at right angles to the given line, and $s/\sqrt{p^2+q^2}$ is the normal distance from the given line to the origin. Since the coordinates (*p, q, s*) for a line are homogeneous, the scaled coordinates $\rho(p, q, s)$, where ρ is any real number, represent the same line. However, for metric computations, such as determining the shortest distance from a line (*p, q, s*) to any point, the line coordinates must be *normalized*, i.e. ρ is chosen so that $1/\rho = \sqrt{p^2+q^2}$. When ρ is negative, the sense of the unit normal is reversed, thereby providing a way to identify that side of a profile which faces inward. For example, the point equations for the two lines in Fig. 5 are $x + 2y \pm 2 = 0$, the upper and lower signs, respectively, applying to lines *A* and *B*. If these were opposite sides of a closed line-profile, an appropriate choice at each line for the sign and magnitude of its normalizing factor ρ would make the signs and

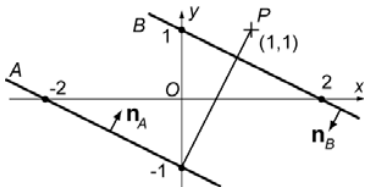

Fig. 5. A point *P* and two lines *A* and *B* in the *xy*-plane, each with its inwardly directed normal $\mathbf{n}_i$.

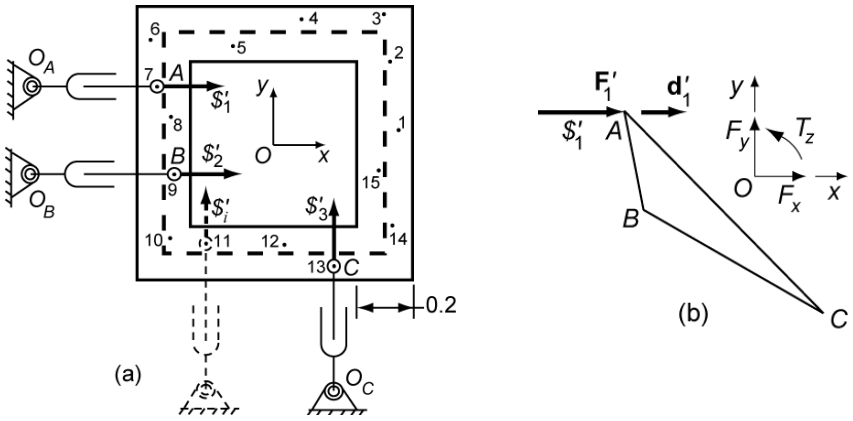

Fig. 6. (a) The line-profile (dashed line) of Fig. 1, its tolerance-zone boundaries (with an exaggerated scale), and 15 measured points, all lying on the platform of a planar in-parallel robot which is guided by three linear actuators lying on the screws $\$'_1$, $\$'_2$ and $\$'_3$ at points *A*, *B*, and *C;* (b) The free-body diagram of the platform carrying the profile when the actuators at $\$'_2$ and $\$'_3$ are unpowered and free. The external loads are the force $\mathbf{F}'_1$ acting along the screw $\$'_1$ at point *A* and the equilibrium wrench ($\mathbf{F}_1$;$\mathbf{T}_1$) exerted on the platform from the environment and represented with the coordinates (*Fx, Fy; Tz*). Also shown is the differential displacement vector $\mathbf{d}'_1$ that is aligned with $\$'_1$ at *A*. The shape of the platform *ABC*, and the relative location of the *xy*-frame are together congruent to those same features in Fig. 6(a).

magnitudes of its *p*- and *q*-coordinates identical to the coordinates for the inward unit normals $\mathbf{n}_A$ or $\mathbf{n}_B$ and make the shortest distance from the line to the origin be equal to *s*. This procedure gives the normalized coordinates for line *A* to be $(p, q, s) = (1, 2, 2)/\sqrt{5}$ and those for line *B* to be $(-1, -2, 2)/\sqrt{5}$, and both distances to the origin become $+s = 2/\sqrt{5}$, the positive sign indicating that the sense of each measurement is consistent with that for its unit normal.

Given a point (*x, y*) and a line (*p, q, s*), both in a planar *xy*-frame, the equation ensuring that the point lies on the line is $px + qy + s = 0$. Further, when the point does not lie on the line, its minimum (normal) distance from the line is [13]

$$d = px + qy + s; \qquad (4)$$

this distance will be in the same units as those for *x* and *y* of a measured point whenever coordinates (*p, q, s*) are scaled so that $p^2 + q^2 = 1$, i.e. when the coordinates are normalized. For instance, the (directed) distance from line *A* in Fig. 5 to point *P* is $(1\cdot1 + 2\cdot1 + 2)/\sqrt{5} = +\sqrt{5}$, and from line *B* it is $-1/\sqrt{5}$.

Assessing minimum distances at the corners of a profile can be problematic because the envelope tangent-lines are not *segments;* instead, each line (*p, q, s*) is of infinite extent. Consider measured point #3 in Fig. 6(a): it lies *on* an envelope-line that is parallel with the *y*-axis, yet its deviation from the theoretical profile should be measured from the higher envelope-line that is horizontal. This matter will be resolved by assessing minimum distances from a *reference-envelope* that is a parallel curve larger than the middle-sized profile. A larger parallel curve is generated easily from the envelope description of a middle-sized profile by increasing the value of coordinate *s* by the same amount for every tangent-line. For purposes of the profile and measured points shown in Fig. 6(a), the outer boundary to the tolerance-zone is an acceptable reference-envelope ($\Delta S = t/2 = 0.1$mm), although a value of $\Delta S = 2t$ or $3t$ is surely better in a practical measurement setting to allow for some measured points to lie outside of the tolerance-zone. Once the correct minimum-distance direction $\mathbf{n}_i$ and a corresponding distance *d* from the reference envelope are established for each point, it is easy to subtract ΔS from every distance value.

5. Least-squares fit of a line-profile to measured points

In Fig. 6(a), the middle-sized profile (dashed line) and the boundaries of its tolerance-zone are shown drawn on the platform of a planar in-parallel robot that is guided with three linear actuators that lie on the normalized screws $\$'_1$, $\$'_2$, and $\$'_3$. The actuators are attached to the platform at three of the measured points, i.e. at *A*, *B*, and *C*, and the directions of the corresponding $\$'_i$ are the same as for the inward unit normals $\mathbf{n}_i$ from the closest side of the square to the (enlarged) reference envelope for the profile. Each of the three linear actuators exerts a force of magnitude F'_i and causes a velocity of magnitude v'_i at the measured point where it is attached to the platform. Since speed and time are of no importance in measurement reduction, each v'_i will be replaced with a differential displacement d'_i of the measured point in the direction of $\mathbf{n}_i$. The corresponding deviation torsor for the platform body is represented by [$] ≡ (0, 0, *δθ; δx, δy,* 0). Since

displacements are confined to the *xy*-plane, the three zero-coordinates may be omitted.

Each of the actuator forces in the *xy*-plane is represented with wrench coordinates, i.e. $F_i'\ \$'_i \equiv (\mathbf{F}'_i;\ \mathbf{T}'_i) \equiv (\mathcal{L}'_i,\ \mathcal{M}_i',\ 0;\ 0,\ 0,\ \mathcal{R}'_i)$, where $\mathcal{L}'_i$ and $\mathcal{M}_i'$ are the *x*- and *y*-components of actuator-force $\mathbf{F}'_i$ and $\mathcal{R}'_i$ is the moment of $\mathbf{F}'_i$ about the origin, i.e. $\mathcal{R}'_i = -y_i\mathcal{L}'_i + x_i\mathcal{M}_i'$. Since all forces will lie in the *xy*-plane, the three zero-coordinates may be omitted, just as for [$]. Also, the geometry may be isolated from the statics by normalizing the wrench coordinates, i.e.

$$F'_i\$'_i \equiv (\mathcal{L}'_i,\ \mathcal{M}'_i\ ;\ \mathcal{R}'_i) \equiv F'_i(L'_i,\ M'_i\ ;\ R'_i), \qquad (5)$$

this making $(L'_i)^2 + (M_i')^2 = 1$. The normalized coordinates L'_i, M_i', and R'_i for each $\$'_i$ are the scalar *screw* coordinates for the actuator-wrench $F_i'\$'_i$; they contain only geometry, i.e. direction and location of $F_i'\$'_i$.

A free-body diagram of the platform in Fig. 6(a) contains the three forces $\mathbf{F}'_i$ (i = 1, 2, 3) and an equilibrium wrench, composed of a force and a couple, exerted on the platform from the environment. The force and couple are represented with the wrench ($\mathbf{F}$; $\mathbf{T}$). Consider now that all of the actuated joints have no force applied and are free to move except one, say $\$'_1$, shown in Fig. 6(b). Then, the only additional loads on a free-body diagram of the platform are those *portions* of the equilibrium wrench reacting back on it from the environment which are required to equilibrate $F_1'\$'_1$, i.e. the force and couple ($\mathbf{F}_1$; $\mathbf{T}_1$) shown in Fig. 6(b) with the components F_x, F_y, and T_z. Since the virtual work of all forces and moments on the free body must be zero for a kinematically admissible displacement of the platform arising from $\mathbf{d}'_i$, the system of forces and couples for the special case in Fig. 6(b) leads to

$$F_1'd'_1 + [T_z\ F_x\ F_y][\delta\theta\ \ \delta x\ \ \delta y]^{\mathsf{T}} = 0, \qquad (6)$$

in which the order of the coordinates in ($\mathbf{F}_1$; $\mathbf{T}_1$) has been changed to ($\mathbf{T}_1$; $\mathbf{F}_1$) and the zero-coordinates again have been omitted. The term $F_1'd'_1$ represents the virtual work of force $\mathbf{F}'_1$ with virtual displacement $\mathbf{d}'_1$, both in the direction of $\$'_1$, at point *A* on the platform. And the product $[T_z\ \ F_x\ \ F_y][\delta\theta\ \ \delta x\ \ \delta y]^{\mathsf{T}}$ represents the virtual work from the equilibrium-wrench ($\mathbf{T}_1$; $\mathbf{F}_1$) acting on the platform whose deviation torsor is $[\$] \equiv [\delta\theta\ \ \delta x\ \ \delta y]^{\mathsf{T}}$.

It is helpful to shift attention to the wrench $-(\mathbf{T}_1\,;\mathbf{F}_1)$ exerted on the environment and *produced* at the platform by the force $F_1'\$'_1$ at *A*. Since the platform in Fig. 6(b) is a two-force (two-wrench) member, with each wrench intensity of equal magnitude, $-(\mathbf{T}_1\,;\mathbf{F}_1) \equiv -(T_z\,;F_x\,,F_y) \equiv (\mathcal{R}'_1\ ;\ \mathcal{L}'_1,\ \mathcal{M}_1') \equiv F_1'\ (R'_1;\ L'_1,\ M_1')$. Making this substitution in Eq. (6) gives

$$F'_1d'_1 = F'_1[R'_1;\ L'_1,\ M'_1][\delta\theta\ \ \delta x\ \ \delta y]^{\mathsf{T}} \qquad (7)$$

for the virtual work expression when force is exerted only at $\$'_1$. Two more Eqs. (7), with subscripts $_2$ and $_3$, occur when force is applied only at $\$'_2$ and only at $\$'_3$, i.e. at points *B* and *C* in Fig. 6(a). The force-amplitude at each actuated joint may be removed from each term, and all terms on the right come from the product of a row matrix and a column matrix of three elements each. When the three equations are ordered sequentially, then the rows of screw coordinates, when taken together, comprise a matrix $[\boldsymbol{K}']$ that is formed entirely from the (normalized) coordinates for $\$'_1$, $\$'_2$ and $\$'_3$, and the three equations may be written

$$\begin{bmatrix} d'_1 \\ d'_2 \\ d'_3 \end{bmatrix} = \begin{bmatrix} R'_1 & L'_1 & M'_1 \\ R'_2 & L'_2 & M'_2 \\ R'_3 & L'_3 & M'_3 \end{bmatrix} \begin{bmatrix} \delta\theta \\ \delta x \\ \delta y \end{bmatrix} \quad \text{or} \quad [\mathbf{d}'_i] = [\boldsymbol{K}'][\$]. \qquad (8)$$

The reader familiar with robotics will recognize $[\boldsymbol{K}']$ as a Jacobian for the actuators of the robot platform in which the normalized coordinates have been rearranged from the usual order that is used for formulating the 'forward force' relationships. (For those interested in a more detailed treatment of the principles involved, the notation here has been made nearly consistent with that in Davidson & Hunt [13], §§1.6, 6.11, 8.5, and 9.6.)

So long as the screws $\$'_1$, $\$'_2$ and $\$'_3$ are independent for the three measured deviations d'_1, d'_2, and d'_3 at locations *A*, *B*, and *C* around the profile, the solution to Eq. (8) for [$], i.e. $[\$] = [\boldsymbol{K}']^{-1}[\mathbf{d}'_i]$, is unique and all three scalar Eqs. (8) are satisfied exactly. This solution ensures that deviations d'_1, d'_2, and d'_3, regarded as small displacements, are kinematically consistent with the platform (profile) displacement [$]. However, in practical situations, there are many more measured points around a line-profile than three. For instance, in Fig. 6(a) there are 15 points. For every additional point, there would be an added, and redundant, linear actuator with its normalized screw $\$'_i$ exerting a force of amplitude F_i' on the platform. One example is shown with dashed lines at Point 11 in Fig. 6(a). Each of these additional points adds a row to the matrices $[\mathbf{d}'_i]$ and $[\boldsymbol{K}']$ in Eq. (8), so that, for all the measured points,

$$[\mathbf{d}'_i] = \begin{bmatrix} d'_1 \\ d'_2 \\ \vdots \\ d'_n \end{bmatrix} = [\boldsymbol{K}'][\$] = \begin{bmatrix} R'_1 & L'_1 & M'_1 \\ R'_2 & L'_2 & M'_2 \\ \vdots & \vdots & \vdots \\ R'_n & L'_n & M'_n \end{bmatrix} [\$], \qquad (9)$$

a result similar to that in Eq. (2) in which $[\boldsymbol{K}']$ there is also a rectangular matrix.

The coordinates ($\delta\theta$, δx, δy) of [$] appear only in a 3-D cross-section of the T-Map (Fig. 3(b)), such as in the base of the 4-D double hyperpyramid in Fig. 4; they do not represent the *size* of the least-squares envelope, i.e. the fourth dimension of the T-Map. The values for measured deviations d'_i, then, may all contain a constant value $-\Delta F$ that represents the change in feature size between that of the middle-sized profile and the least-squares profile, and they *must* contain a value ΔS that was introduced artificially in §4 to establish the correct proximity of a measured point to the profile. For reduction of CMM data, then, each generic Eq (7) must be augmented to

$$\left.\begin{aligned} d'_i &= [R'_i\ L'_i\ M'_i][\delta\theta\ \ \delta x\ \ \delta y]^{\mathrm{T}} + (\Delta S - \Delta F) \\ &= [R'_i\ L'_i\ M'_i\ 1][\delta\theta\ \ \delta x\ \ \delta y\ \ \ (\Delta S - \Delta F)\ ]^{\mathrm{T}} \end{aligned}\right\} \qquad (10)$$

(compare to $y_i = mx_i + b$ in §2). The size-change ΔF is introduced in Eq. (11) with a negative sign because all the d'_i-values are directed inward in Fig. 6, corresponding to a *reduction* in size. Yet the 4-D T-Map in Fig. 4 is arranged with the rightward sense, a more natural positive sense, corresponding to *increase* in size, i.e. from the smallest (ψ_1) to the largest (ψ_2) profile allowable in the tolerance-zone.

The scalar relation in Eq (10) forms the transition between the setting of in-parallel robotics and the setting of reducing CMM data to geometric variables related to Tolerance-Maps. Now the least-squares fit is obtained by minimizing the sum

$$\sum[\, d'_i - \{\, R'_i\delta\theta + L'_i\delta x + M'_i\delta y + (\Delta S - \Delta F)\}\,]^2 \qquad (11)$$

for $i = 1\ldots n$. Matrix [$] in Eq (9) is augmented to contain the *four* components $\delta\theta$, δx, δy and $(\Delta S - \Delta F)$, and the matrix $[\boldsymbol{K}']$ in Eq (9) is augmented on the right with a column of ones so that the n Eqs (10) (for the n measured points) produce the matrix equation

$$[\mathbf{d}'_i] = \begin{bmatrix} d'_1 \\ d'_2 \\ \vdots \\ d'_n \end{bmatrix} = [\boldsymbol{K}'][\$] = \begin{bmatrix} R'_1 & L'_1 & M'_1 & 1 \\ R'_2 & L'_2 & M'_2 & 1 \\ \vdots & \vdots & \vdots & \vdots \\ R'_n & L'_n & M'_n & 1 \end{bmatrix}[\$]. \qquad (12)$$

The Moore-Penrose solution to Eq. (9) for [$], i.e. $[\$] = [\boldsymbol{K}']^{\#}[\mathbf{d}'_i]$ (see Eq. (3)), produces the least-squares location ($\delta\theta$, δx, δy) and size-adjustment ($\Delta S - \Delta F$) for the profile [9], i.e. that location and size for a profile which minimizes the sum in Eq (11). (Compare the pair of Eqs (1) and (2) to the pair (11) and (12).) Note that, when $\delta\theta$ is modified to $\overline{a}\ \delta\theta$, the i-Map-coordinates ($\overline{a}\ \delta\theta$, δx, δy, ΔF) represent (θ', e_x, e_y, ΔF) in the coordinates of the T-Map of Fig. 4.

6. Example

As one numerical example, consider the measured points that are shown around the middle-sized profile in Fig. 6(a). The points represent an imperfectly manufactured square profile. The coordinates (L'_1, M_1'; R'_1) for the actuator screws at each point, and the deviations d', are presented in Table 2 for each of the measured points; the deviations are all measured from the outer boundary of the tolerance-zone, so $\Delta S = 0.1$ mm (Fig. 3(a)). The values in Table 2 are used to build matrices $[\boldsymbol{K}']$ and $[\mathbf{d}'_i]$ in Eq. (12). The Moore Penrose solution of $[\boldsymbol{K}']$ produces the least-squares solution

$$[\$] = [\delta\theta\ \ \delta x\ \ \delta y\ (\Delta S - \Delta F)]^{\mathrm{T}}$$

$$= [0.000562\ \ 0.011858\ \ 0.013294\ \ 0.092828]^{\mathrm{T}}.$$

Table 2. Coordinates of measured points around a manufactured square profile

Points	L'_i	M_i'	R'_i, mm	d_i', mm
1	–1	0	5	0.05
2	–1	0	30	0.08
3	0	–1	–40	0.02
4	0	–1	–10	0.05
5	0	–1	15	0.15
6	1	0	–38	0.05
7	1	0	–20	0.08
8	1	0	–10	0.12
9	1	0	11	0.14
10	1	0	35	0.12
11	0	1	–25	0.14
12	0	1	4	0.13
13	0	1	22	0.05
14	–1	0	–30	0.08
15	–1	0	–10	0.11

The resultant least-squares profile corresponding to this solution is shown as the profile with the thin line in Fig 7. Note that the scale of the tolerance-zone is enlarged by a factor of 10 in Figs. 6(a) and 7, and the

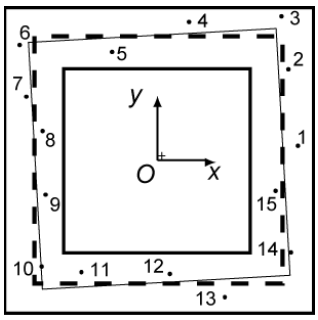

Fig. 7. The resultant least-squares profile shown with the thin line. Its displacement from origin O is shown with the '+' mark.

scale for the profile dimensions is diminished by a factor of 10. Consequently, the least-squares profile is drawn at $\delta\theta$ = 0.0562 rad = 3.22° in the counterclockwise direction. Further, to make the appearance of the displaced origin '+' in Fig. 7 be consistent with the displayed points, its coordinates δx = 0.011858 mm and δy = 0.013294 mm have been scaled up by a factor of 10 with respect to the middle-sized profile. The corresponding size adjustment from the middle-sized profile is ΔF = 0.1 – 0.092828 = 0.007172 mm, a small *growth* in size. And, finally, the coordinates (e_x, e_y, θ', ΔF) of the *i*-Map point, corresponding to the above solution, are, respectively, 0.011858 mm, 0.013294 mm, 0.02248 mm, and 0.007172 mm, when rounded to three significant figures. Coordinate $\theta' = \overline{a}\ \delta\theta = 40\,\delta\theta$ for the line-profile in Fig. 1.

7. Conclusion

The method in this paper is an alternative to the one proposed in [6]: both techniques provide a rigid body transformation that locates a set of points that have been measured on a profile relative to a specified tolerance-zone. In [6] a minimum-zone capture of the points is computed, whereas here the least-squares fit of the points is utilized. However, in this paper another variable is added to the computed results, the size of the profile, so identifying a corresponding point (*i*-Map) within the T-Map of tolerance specifications in Fig. 4. Although the least-squares fit is just one of several possible fits to measured points, it is an important one because it recognizes (a) the inter-penetration of mating surfaces (asperities), which violate computed minimum-zone boundaries, and (b) the potential existence of other points further from the intended feature than any of the measured ones. Any one such point could noticeably change a computed minimum zone, but it would have little effect on a least-squares computation that is based on a large number of measured points. And, of course, a minimum-zone may be constructed from the least-squares solution by forming parallel inner and outer boundaries that capture all the measured points.

Acknowledgements

The authors are grateful for funding provided by National Science Foundation Grant #CMMI-0969821.

References

[1] American National Standard ASME Y14.5M. *Dimensioning and Tolerancing*, New York: The American Society of Mechanical Engineers 2009.

[2] Mani N, Shah JJ, Davidson JK. Standardization of CMM fitting algorithms and development of inspection maps for use in statistical process control. *Proc. ASME 2011 International Manufacturing Science and Engineering Conference, Volume 2*, Corvallis, Oregon, USA, June 13–17, 2011. Paper #MSEC2011-50152.

[3] Choi W, Kurfess TR. Dimensional measurement data analysis, part 1: A zone fitting algorithm. *J Manuf Sci Eng* 1999; **121**:238-245.

[4] Carr K, Ferreira P. Verification of form tolerances part I: Basic issues, flatness, and straightness. *Precision Engineering* 1995; **17**: 131-143.

[5] Carr K, Ferreira P. Verification of form tolerances part II: Cylindricity and straightness of a median line. *Precision Engineering* 1995; **17**: 144-156.

[6] Choi W, Kurfess TR. Dimensional measurement data analysis, part 2: Minimum zone evaluation. *J. Manuf. Sci. Eng.* 1999;**121**:246-250.

[7] Barari A, ElMaraghy HA, Knopf GK. Evaluation of Geometric Deviations in Sculptured Surfaces Using Probability Density Estimation. *Models for Computer-Aided Tolerancing in Design and Manufacturing* (ed. J. K. Davidson), (Proc., 9th CIRP Int'l Seminar on CAT, April 10-12, 2005, Tempe, AZ, USA). Dordrecht, Netherlands: Springer 2007:45-54.

[8] Choi SC. *Introductory applied statistics in science*, Englewood Cliffs, NJ: Prentice-Hall 1978, p. 23-35.

[9] Ben-Israel A, Greville TNE. *Generelized inverse: Theory and application 2nd ed.*, New York: Springer 2003.

[10] Davidson JK, Shah JJ. *Modeling of geometric variations for line-profiles*. In press for *ASME Transactions, J. of Computing & Information Science in Engrg*. 2012; **12**: 9 pp.

[11] Coxeter HSM. *Introduction to geometry*. 2nd ed., Wiley Classic Library 1969.

[12] Hain, K. *Applied kinematics*. 2nd ed., McGraw-Hill 1967.

[13] Davidson JK, Hunt KH. *Robots and screw theory. Application of kinematics and statics to robotics*, Oxford: Oxford University Press 2004.